

Anisotropy of the upper critical field in superconductors with anisotropic gaps. Anisotropy parameters of MgB₂

P. Miranović and K. Machida

Department of Physics, Okayama University, 700-8530 Okayama, Japan

V. G. Kogan

Ames Laboratory DOE and Physics Department ISU, Ames, IA 50011, USA.

The upper critical field H_{c2} is evaluated for weakly-coupled two-band anisotropic superconductors. By modeling the actual bands and the gap distribution of MgB₂ by two Fermi surface spheroids with average parameters of the real material, we show that $H_{c2,ab}/H_{c2,c}$ increases with decreasing temperature in agreement with available data.

PACS numbers: 74.60.Ec, 74.20.-z, 74.70.Ad

The anisotropic Ginzburg-Landau (GL) equations, derived for clean superconductors with arbitrary gap anisotropy by Gor'kov and Melik-Barkhudarov [1], led to a common practice of characterizing materials by a single anisotropy parameter defined as $\xi_a/\xi_c \equiv \lambda_c/\lambda_a$ (ξ is the coherence length, λ is the penetration depth, and a, c are principal directions of a uniaxial crystal of the interest here). Formally, this came out because in the GL domain, the same “mass tensor” determines the anisotropy of both ξ (of the upper critical fields H_{c2}) and of λ .

At arbitrary temperatures, however, the ratios of H_{c2} 's and of λ 's are not necessarily the same. We demonstrate below that in materials with anisotropic Fermi surfaces and anisotropic gaps, not only $H_{c2,a}/H_{c2,c}$ may strongly depend on T , but this ratio might differ considerably from λ_c/λ_a at low T 's. Our arguments are based on the weak-coupling model of superconductivity for simple Fermi surfaces and gap anisotropies; as such they are at best qualitative. Still, being applied to MgB₂, they provide satisfactory description of existing data for the H_{c2} anisotropy.

There are two different approaches in literature in describing macroscopics of the “two-gap” superconductivity of MgB₂. One of these treats the anisotropy of interaction by introducing a coupling matrix ρ_{ij} for intra- and interband pair transfer. Various relations between the matrix elements yield variety of macroscopic consequences. One of the realizations of the model considers two order parameters with two distinct phases which may lead to various static [2, 3] and dynamic [4] effects. Certain relations between elements ρ_{ij} provide the experimentally observed gaps and their ratio. The approach adopted in this paper considers the gap on two Fermi sheets just as a particular case of the gap anisotropy, the gap ratio being the experimental input parameter. Within this scheme, there is only one complex order parameter Ψ , a single critical temperature T_c is built in, and the number of input parameters needed for calculations is small. The resulting H_{c2} 's of these two approaches are similar [5]. Our choice is dictated by theoretical simplic-

ity, rather than by experimental necessity.

Below, the general scheme of calculating $H_{c2}(T)$ based on the Eilenberger method [6] is outlined for both the gap and the Fermi surface being anisotropic [7]. Then, we estimate the H_{c2} anisotropy of MgB₂ by modeling the four-sheet Fermi surface as calculated in Refs. 8, 9, 10 with the gap distribution having two sharp maxima, by two distinct Fermi sheets $F_{1,2}$ with gaps $\Delta_{1,2}$, each being constant within its sheet. Since the actual band structure enters macroscopic superconducting parameters via Fermi-surface averages, we further model the sheets $F_{1,2}$ by two spheroids with average Fermi velocities close to the band-structure generated values. As a result we obtain qualitatively (and - given the spread of existing data - quantitatively) correct behaviors of $H_{c2}(T)$ for both principal directions.

A clean weakly coupled superconductor at $H_{c2}(T)$ is described within the quasiclassical Eilenberger scheme by the anomalous Green's function $f(\omega, \mathbf{v}, \mathbf{r})$, which satisfies an equation:

$$(2\omega + \mathbf{v}\mathbf{\Pi})f = 2\Delta/\hbar. \quad (1)$$

Here, \mathbf{v} is Fermi velocity; $\omega = \pi T(2n + 1)/\hbar$ are the Matsubara frequencies; $\mathbf{\Pi} = \nabla + (2\pi i/\phi_0)\mathbf{A}$ with the vector potential \mathbf{A} and the flux quantum ϕ_0 . The Eilenberger function g describing normal excitations, is unity at $H_{c2}(T)$. Equation (1) holds for any Fermi surface and gap anisotropies.

The gap function Δ satisfies the self-consistency equation:

$$\Delta(\mathbf{r}, \mathbf{v}) = 2\pi T N(0) \sum_{\omega > 0}^{\omega_D} \langle V(\mathbf{v}, \mathbf{v}') f(\omega, \mathbf{v}', \mathbf{r}) \rangle_{\mathbf{v}'} . \quad (2)$$

Here, $\langle \dots \rangle$ denotes the average over the Fermi surface. The pair scattering potential V is assumed factorizable, $V(\mathbf{v}, \mathbf{v}') = V_0 \Omega(\mathbf{v}) \Omega(\mathbf{v}')$, with the function $\Omega(\mathbf{v})$ normalized so that

$$\langle \Omega^2 \rangle = 1. \quad (3)$$

Further, we look for $\Delta(\mathbf{r}, T; \mathbf{v}) = \Psi(\mathbf{r}, T) \Omega(\mathbf{v})$ [11], the form implying a one-component order parameter. Then, after excluding V_0 with the help of the BCS formula for T_c , one arrives to Eq. (2) of the form:

$$\frac{\Psi}{2\pi T} \ln \frac{T_c}{T} = \sum_{\omega>0}^{\infty} \left(\frac{\Psi}{\hbar\omega} - \langle \Omega f \rangle \right) \quad (4)$$

(for more details and references see, e.g., Ref. 12).

The linear Eq. (1) is inverted:

$$f = \frac{2}{\hbar} (2\omega + \mathbf{v}\Pi)^{-1} \Delta = \frac{2\Omega}{\hbar} \int_0^{\infty} d\rho e^{-\rho(2\omega + \mathbf{v}\Pi)} \Psi. \quad (5)$$

In the GL domain, the gradients $\Pi \sim \xi^{-1} \rightarrow 0$, and one can keep in the expansion of $\exp(-\rho\mathbf{v}\Pi)$ only the terms up to the second order. Then, Eq. (4) yields:

$$-\Psi\delta t = \frac{7\zeta(3)\hbar^2}{16\pi^2 T_c^2} \langle \Omega^2 (\mathbf{v}\Pi)^2 \Psi \rangle, \quad (6)$$

where $\delta t = 1 - T/T_c$. This is the anisotropic linearized GL equation of Ref. 1:

$$-\xi_{ik}^2 \Pi_i \Pi_k \Psi = \Psi, \quad \xi_{ik}^2 = \frac{7\zeta(3)\hbar^2}{16\pi^2 T_c^2 \delta t} \langle \Omega^2 v_i v_k \rangle. \quad (7)$$

The anisotropy parameter in this domain follows:

$$\gamma_H^2(T_c) = \frac{H_{c2,a}^2}{H_{c2,c}^2} = \frac{\xi_{aa}^2}{\xi_{cc}^2} = \frac{\langle \Omega^2 v_a^2 \rangle}{\langle \Omega^2 v_c^2 \rangle}. \quad (8)$$

It should be stressed that at T_c , the anisotropy of the London penetration depth $\gamma_\lambda(T_c) = \lambda_c/\lambda_a$ is determined by the same tensor $\langle \Omega^2 v_i v_k \rangle$, i.e., $\gamma_\lambda(T_c) = \gamma_H(T_c)$, see Refs. 1 or 12.

The formal method. To treat arbitrary T 's, we follow Helfand-Werthamer's routine [13] (for Eilenberger based procedure see, e.g., Refs. 7, 14): introduce $v^\pm = v_x \pm i v_y$ and $\Pi^\pm = \Pi_x \pm i \Pi_y$ for the field along z , write $\mathbf{v}\Pi = (v^+ \Pi^- + v^- \Pi^+)/2$, and use known properties of exponential operators to evaluate $\exp(-\rho\mathbf{v}\Pi)$. There are a few ways to proceed with actual calculation. E.g., by writing $\omega^{-1} = 2 \int_0^\infty d\rho e^{-2\rho\omega}$, one can sum up over ω in Eq. (4) and evaluate numerically the remaining integrals over ρ . We found it a faster procedure to follow Rieck and Scharnberg [7]: first to express integrals over ρ in terms of Repeated Integrals of the Error Function $\text{i}^n \text{erfc}(x)$ [15], and then numerically evaluate convergent sums over ω . We then obtain:

$$f = \frac{\Omega}{\hbar} \sqrt{\frac{2\phi_0}{H}} \sum_{n,m=0}^{\infty} I_{nm} (\hat{a}^+)^m (\hat{a}^-)^n \Psi, \quad (9)$$

$$I_{nm} = \frac{(n+m)!}{n!m!} \left(i\sqrt{2} \right)^{n+m} \frac{(v^-)^{m-n}}{v_\perp^{m-n+1}} \text{i}^{n+m} \text{erfc}(x) e^{x^2},$$

where $\hat{a}^\pm = i\sqrt{\phi_0/4\pi H} \Pi^\pm$, $x = (\omega/v_\perp)\sqrt{2\phi_0/\pi H}$ and $v_\perp^2 = v_x^2 + v_y^2$.

To satisfy the self-consistency equation we expand Ψ in a complete set of functions Ψ_j constructed by Eilenberger to represent various vortex lattice solutions:

$$\Psi = \sum_{j=0}^{\infty} C_j \Psi_j. \quad (10)$$

In fact, we do not need the explicit form of Ψ_j (they can be found in Ref. 16); suffices it to mention that Ψ_0 has the known Abrikosov form, whereas the rest are found by applying \hat{a}^+ to Ψ_0 : $\hat{a}^+ \Psi_n = \sqrt{n+1} \Psi_{n+1}$ and $\hat{a}^- \Psi_n = \sqrt{n} \Psi_{n-1}$. After some algebra, we arrive at the following equation:

$$\sum_{\omega>0} \sum_{j,m} \sum_{n=0}^j \langle \Omega^2 I_{nm} \rangle \frac{\sqrt{j!(j-n+m)!}}{(j-n)!} C_j \Psi_{j-n+m} = \frac{\hbar\sqrt{H}}{2\pi T \sqrt{2\phi_0}} \left(\ln \frac{T}{T_c} + 2\pi T \sum_{\omega>0} \frac{1}{\hbar\omega} \right) \sum_{j=0}^{\infty} C_j \Psi_j. \quad (11)$$

As argued in Ref. 7, the integers j and $n-m$ should be taken even. When the coefficients in front of each Ψ_k are set zero, the homogeneous system of linear equations for C_k is obtained. The determinant of this system has to be zero, which gives an equation for H ; the highest root is the upper critical field.

MgB₂. The band structure calculations show that the Fermi surface of this material consists of sheets coming from two π -bands and two quasi-two-dimensional σ -bands [8, 9, 10]. It has been shown by solving the Eliashberg equations [9, 10] that the gap on the four Fermi surface sheets has two sharp maxima: $\Delta_1 \approx 1.7 \text{ meV}$ at the two π -bands and $\Delta_2 \approx 7 \text{ meV}$ at the two σ -bands. Within each of these groups, the spread of the gap values is small, and the gaps can be considered as constants, the ratio of which is nearly T independent. Experimental estimates of the mean-free path ℓ show that in most of available samples $\ell \gg \xi(0)$, i.e., the material can be considered as a clean superconductor.

The macroscopic anisotropies such as those of H_{c2} , of the penetration depth λ , of the magnetization, etc., are determined within a weak-coupling theory by the Fermi surface averages [see, e.g., Eqs. (7) and (8)]. Therefore, for qualitative study of these anisotropies, fine details of the Fermi surfaces are unlikely to be relevant. We then *model* the Fermi surface of this material as two separate sheets F_1 and F_2 with average characteristics taken from actual band structure results. Thus, we consider a model material with the gap anisotropy given by

$$\Omega(\mathbf{v}) = \Omega_{1,2}, \quad \mathbf{v} \in F_{1,2}. \quad (12)$$

Denoting the densities of states on the two parts as $N_{1,2}$,

we obtain for the general averaging:

$$\langle X \rangle = \frac{N_1 \langle X_1 \rangle + N_2 \langle X_2 \rangle}{N(0)} = \nu_1 \langle X_1 \rangle + \nu_2 \langle X_2 \rangle, \quad (13)$$

where $N(0)$ is the total density of states and we introduced normalized densities of state $\nu_{1,2}$ for brevity. We have then instead of Eq. (3):

$$\Omega_1^2 \nu_1 + \Omega_2^2 \nu_2 = 1, \quad \nu_1 + \nu_2 = 1. \quad (14)$$

We also assume that the two parts of the Fermi surface have the symmetries of the total, e.g., $\langle \mathbf{v} \rangle_1 = 0$ where the average is performed only over the first Fermi sheet.

According to Refs. 8, 9, the relative densities of states ν_1 and ν_2 of our model are ≈ 0.56 and 0.44 . The ratio $\Delta_2/\Delta_1 = \Omega_2/\Omega_1 \approx 4$, if one takes the averages of 6.8 and 1.7 meV for the two groups of distributed gaps as calculated in Ref. 9. Then, the normalization (14) yields $\Omega_1 = 0.36$ and $\Omega_2 = 1.45$. One should have in mind that the data on the gaps ratio vary from less than 3 (see, e.g., [17] and references therein) to more than 4 [18].

In the following we use averages over separate Fermi sheets calculated in Ref. 8: $\langle v_a^2 \rangle_1 = 33.2$, $\langle v_c^2 \rangle_1 = 42.2$, $\langle v_a^2 \rangle_2 = 23$, and $\langle v_c^2 \rangle_2 = 0.5 \times 10^{14} \text{ cm}^2/\text{s}^2$. It is worth noting that the ratio $\langle v_a^2 \rangle / \langle v_c^2 \rangle$ is 0.79 for F_1 , and 46 for F_2 , whereas for the whole Fermi surface it is 1.2.

We further model the pieces $F_{1,2}$ by spheroids, in other words, we consider quadratic energy spectra $E_\mu(\mathbf{k}) = (k_x^2 + k_y^2)/(2m_{a,\mu}) + k_z^2/(2m_{c,\mu})$, $\mu = 1, 2$. Within this simple model, evaluation of averages is tedious yet straightforward; to get the averages given above we need $m_{a,1}/m_{c,1} = 1.3$ and $m_{a,2}/m_{c,2} = 0.029$.

The expansion (10) converges fast at high T 's, but we need terms up to Ψ_{20} to stabilize the low temperature values of $H_{c2,a}$. The temperature dependence of H_{c2} for two principal directions so calculated is shown in Fig. 1. The curve $H_{c2,c}(T)$ is similar to that of Helfand-Werthamer [13], the result confirmed by the data of Ref. 19. On the other hand, $H_{c2,a}$ has a slight positive curvature at high temperatures. As a result, the ratio $H_{c2,a}/H_{c2,c}$ is temperature dependent, as shown by the upper curve of Fig. 2.

It is of interest to note that within a few %, solutions Ψ of the self-consistency Eq. (11) can be approximated by solutions of $-\xi_{ik}^2 \Pi_i \Pi_k \Psi = \Psi$, with properly chosen parameter $\gamma_H(T) = \xi_a/\xi_c$. The reasons for this will be discussed elsewhere [5]. Physically, this means that the angular dependence of H_{c2} at any T should be close to:

$$H_{c2}(\theta, T) = \frac{H_{c2,ab}}{\sqrt{\gamma_H^2(T) \cos^2 \theta + \sin^2 \theta}}, \quad (15)$$

where θ is the angle between the applied field and the c axis. This angular dependence has, in fact, been recently reported [20].

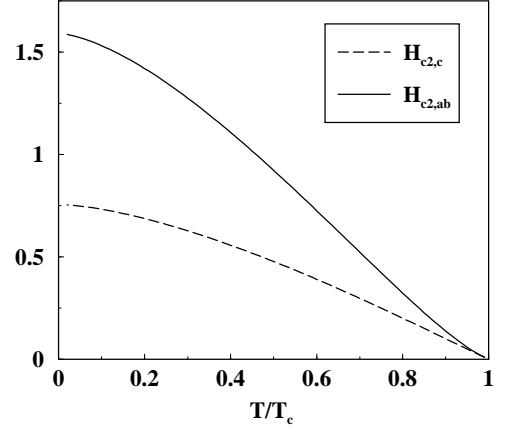


FIG. 1: Temperature dependence of the upper critical field for two principal directions. Note: each field is normalized on its own slope at T_c : $T_c(dH_{c2}/dT)_{T_c}$.

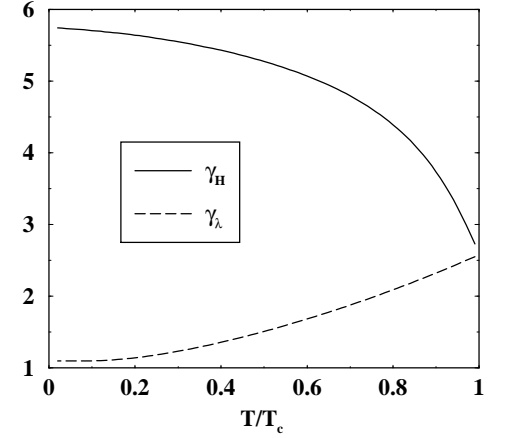


FIG. 2: Anisotropy ratio $\gamma_H = H_{c2,ab}/H_{c2,c}$ versus T/T_c calculated with parameters for MgB_2 given in the text. Dashed line is $\gamma_\lambda(T) = \lambda_c/\lambda_{ab}$ calculated as in Ref. 12.

The drop of the H_{c2} anisotropy with increasing T has been recorded by Angst *et al.* in measurements on single crystals of MgB_2 [21]. Bud'ko and Canfield used a robust method of extracting the anisotropy of H_{c2} [22] in the whole temperature range using the T dependence of the magnetization of random powders [23]. Recent specific heat measurements of Lyard *et al.* [20] and magnetization data of Welp *et al.* [24] on single crystals produced similar results. All these data show qualitatively similar behavior to that of the upper curve of Fig. 2.

Physically, the large anisotropy of H_{c2} at low temperatures (≈ 6 in our calculation) is related to the large gap value at the Fermi sheet which is nearly two-dimensional. With increasing T , the thermal mixing with the small-gap states on the three-dimensional Fermi sheet suppresses the anisotropy down to 2.6 at T_c .

It is worth to compare here the H_{c2} anisotropy with the anisotropy of the penetration depth $\gamma_\lambda(T) = \lambda_c/\lambda_a$

calculated within the same model of MgB_2 [12]. The result is shown by the dashed line in Fig. 2. At T_c , the H_{c2} anisotropy γ_H coincides with γ_λ , as they should because the GL theory contains only one “mass tensor” which determines anisotropies of both ξ^{-2} and λ^2 . The expression (8) for the anisotropy ratio clearly amplifies the contribution of Fermi surface parts with the large gap. However, in a clean material at $T = 0$, the superfluid of Cooper pairs is Galilean invariant; this implies that all charged particles participate in the superflow, their energy spectrum notwithstanding. This is reflected in the result for the λ -anisotropy at $T = 0$,

$$\gamma_\lambda^2(0) = \frac{\langle v_a^2 \rangle}{\langle v_c^2 \rangle}, \quad (16)$$

neither the gap nor its anisotropy enter this expression. As mentioned, for MgB_2 , the ratio (16) is 1.2, i.e., $\gamma_\lambda(0) = 1.1$ in a striking difference with the large zero- T anisotropy of H_{c2} .

Thus, the question “what is the anisotropy parameter of MgB_2 ?” does not have a unique answer. To pose the question properly one should specify the quantity of interest. If this is H_{c2} , the answer is given by the upper curve of Fig. 2 for a clean material; if this is λ , see the dashed line. If this is the magnetization in intermediate fields, $M \propto (\phi_0/\lambda^2) \ln(H_{c2}/H)$, the main contribution to anisotropy comes from λ , however, the H_{c2} anisotropy contributes as well (being smoothed by the logarithm). The last situation should be taken into account while extracting anisotropy from the torque data in tilted fields [25, 26], the point stressed by Angst [27].

Given the simplifying assumptions about the Fermi surfaces we have made and our results for the H_{c2} anisotropy which reproduce qualitatively well the measured anisotropy, we believe that the anisotropic properties of H_{c2} and λ we have described, are generic for materials with anisotropic gaps and Fermi surfaces.

-
- [1] L. P. Gor’kov and T. K. Melik-Barkhudarov, Sov. Phys. JETP, **18**, 1031 (1964).
 [2] A. A. Golubov, and I. I. Mazin, Physica C **243**, 153 (1995).

- [3] I. N. Askerzade, A. Gencer, N. Güclü, and A. Kiliç, cond-mat/0201112.
 [4] A. Gurevich and V. Vinokur, unpublished.
 [5] P. Miranović, K. Machida, and V. G. Kogan, unpublished.
 [6] G. Eilenberger, Z. Phys. **214**, 195 (1968).
 [7] C. T. Rieck and K. Scharnberg, Physica B **163**, 670 (1990).
 [8] K. D. Belashchenko, M. van Schilfgaarde, and V. P. Antropov, Phys. Rev. B **64**, 092503 (2001).
 [9] H. J. Choi, D. Roundy, H. Sun, M. L. Cohen, and S. G. Louie, cond-mat/0111183.
 [10] A. Y. Liu, I. I. Mazin, and J. Kortus, Phys. Rev. Lett. **87**, 087005 (2001).
 [11] V. L. Pokrovsky, Sov. Phys. JETP **13**, 447 (1961).
 [12] V. G. Kogan, Phys. Rev. B **66**, in press (2002).
 [13] E. Helfand and N. R. Werthamer, Phys. Rev. **147**, 288 (1966).
 [14] V. G. Kogan, Phys. Rev. B **26**, 88 (1982).
 [15] *Handbook of Mathematical Functions*, edited by M. Abramowitz and I. A. Stegun, Natl. Bur. Stand. Appl. Math. Ser. No. 55 (U.S. GPO, Washington, D.C., 1965).
 [16] G. Eilenberger, Phys. Rev. **164**, 628 (1967).
 [17] F. Bouquet, Y. Wang, R. A. Fisher, D. G. Hinks, J. D. Jorgensen, A. Junod, and N. E. Phillips, Europhys. Lett. **56**, 856 (2001).
 [18] M. H. Badr and K.-W. Ng, cond-mat/0206391.
 [19] A. V. Sologubenko, J. Jun, S. M. Kazakov, J. Karpinski, and H. R. Ott, Phys. Rev. B **65**, 180505(R) (2002).
 [20] L. Lyard, P. Samuely, P. Szabo, C. Marcenat, T. Klein, K. H. P. Kim, C. U. Jung, H.-S. Lee, B. Kang, S. Choi, S.-I. Lee, L. Paulius, J. Marcus, S. Blanchard, A. G. M. Jansen, U. Welp, and W. K. Kwok, cond-mat/0206231.
 [21] M. Angst, R. Puzniak, A. Wisniewski, J. Jun, S. M. Kazakov, J. Karpinski, J. Roos, and H. Keller, Phys. Rev. Lett. **88**, 167004 (2002).
 [22] S. L. Bud’ko, V. G. Kogan, and P. C. Canfield, Phys. Rev. B **64**, 180506 (2001).
 [23] S. L. Bud’ko and P. C. Canfield, Phys. Rev. **65**, 212501 (2002).
 [24] U. Welp, G. Karapetrov, W. K. Kwok, G. W. Crabtree, Ch. Marcenat, L. Paulius, T. Klein, J. Marcus, K. H. P. Kim, C. U. Jung, S.-S. Lee, B. Kang, and S.-I. Lee, cond-mat/0203337.
 [25] K. Takahashi, T. Atsumi, N. Yamamoto, M. Xu, H. Kitazawa, and T. Ishida, Phys. Rev. B **66**, 012501 (2002).
 [26] G. K. Perkins, J. Moore, Y. Bugoslavsky, L. F. Cohen, J. Jun, S. M. Kazakov, J. Karpinski, and A. D. Caplin, cond-mat/0205036.
 [27] M. Angst, private communication.